JOURNAL OF APPLIED ELECTROCHEMISTRY 17 (1987) 589–599

Textural and structural studies on nickel hydroxide electrodes. II. Turbostratic nickel (II) hydroxide submitted to electrochemical redox cycling

A. DELAHAYE-VIDAL, M. FIGLARZ*

Université de Picardie, Laboratoire de Réactivité et de Chimie des Solides (UA CNRS 1211), 33 rue Saint Leu, F-80039 Amiens Cedex, France

Received 10 April 1986; revised 10 June 1986

The textural and structural modifications involved in electrochemical redox cycling of turbostratic nickel (II) hydroxide has been investigated using X-ray diffraction and electron microscopy methods. It was found that during the first cycles, different phenomena compete: redox reactions which occur in the solid state, and ageing reactions via the solution. For the first galvanostatic charge performed at the C/5 rate in 4.5 N KOH, the direct oxidation of α(II) to γ(III) and the ageing of α(II) to β(II) via the solution followed by the oxidation to γ(III) are in competition. The study of the discharge mechanism shows that the direct reduction γ(III) $\rightarrow$ β(II) is parallel to the reduction γ(III) $\rightarrow$ α(II) and the ageing of the turbostratic hydroxide via the solution. After the first cycle it was established that the alpha-generated β(II) active phase consisted of a mixture of two kinds of particles, the oxidation of which follows two paths: β(II)/β(III) for the thicker particles and for the thinner β(II)/γ(III), but these latter β(II) particles aged via the solution by Oswald ripening and the β(II)/γ(III) couples swung to β(II)/β(III).

1. Introduction

The mechanism of operation of nickel hydroxide electrodes used in the nickel–cadmium battery is a matter of considerable study and controversy. Many studies have dealt with the electrochemical behaviour of the electrode: experimental methods such as potential sweeps and potentiostatic pulses are usually employed to obtain kinetic and thermodynamic data. Nevertheless, an important feature has often been neglected, i.e. the textural characterization of the phases involved in the nickel hydroxide electrode and their evolution during cycling.

So far, no correlation has been shown to exist between textural development and electroactivity of the phases. As a new approach to the chemical and electrochemical redox behaviour of the so-called α- and β-nickel (II) hydroxides, particular emphasis has been placed on the textural and structural modifications of the phases involved in these systems.

In an earlier paper [1] the behaviour of β-type hydroxides as starting active materials has been studied. The existence of important textural modifications was established during the first oxidation cycle. Starting from β(II) nickel hydroxide with a monolithic texture, the formation of a mosaic texture occurs. This mosaic texture is preserved during the first reduction and further cycling. A model based on the pseudomorphous and topotactic characteristics of the reactions involved was used to explain the formation of the mosaic texture. The reactions which take place in the solid state by oriented growth of β(III) or γ(III) on β(II) induce strains within the particles; they are due to the large differences in the nickel–nickel distances in the

* To whom correspondence should be addressed.

0021–891X/87 $03.00 + .12

oxidized and reduced phases. Strain relaxation brings about the formation of a mosaic texture which gives the particles elastic properties that minimize further strains and make their relaxation easier. The formation of this mosaic texture can be related to the well-known forming process of the electrode and its maintenance during cycling can be related to the life cycle performance of the system.

The present paper examines the behaviour of an α-type hydroxide. These α phases can still be considered as nickel (II) hydroxides, but contain a variable excess of water and possibly foreign ions in the interlamellar space between the nickel hydroxide planes and they exhibit disordered structures. The conventional α-$Ni(OH)_2$ denomination used for such compounds must be taken as a general denomination for a large set of degenerate forms of nickel (II) hydroxides or nickel (II) hydroxy-salts [2] and does not represent a well-defined polymorph of nickel hydroxide $Ni(OH)_2$. However, the similarity of trends observed in the electrochemical behaviour of such compounds has induced electrochemists to adopt the same α–β dichotomy as crystallographers and we shall thus adhere to such a convention in the present paper. Nevertheless, the α-type hydroxide considered in this paper is a well-defined hydrated turbostratic hydroxide prepared by chemical precipitation with specific characteristics, as opposed to the α phases obtained by cathodic deposition upon electrolysis of a nickel salt solution; we will denote this phase obtained by chemical precipitation as αc.

The α phases have potential as active materials for nickel hydroxide electrodes. Indeed, it is well known that α-hydroxide, on oxidation, is converted to γ-NiOOH at a lower potential than the corresponding oxidation of β(II) $Ni(OH)_2$ to β(III) NiOOH. Since γ-NiOOH has a higher average nickel oxidation state compared with β-NiOOH [3–7], the capacity of the α/γ system is better than that of β(II)/β(III). Unfortunately, complicating features are that α-hydroxide reverts to β-$Ni(OH)_2$ on standing in alkali [8–10].

In order to enhance our understanding of these phenomena, a study of the turbostratic nickel (II) hydroxide material αc submitted to electrochemical redox cycling has been carried out.

2. The turbostratic nickel (II) hydroxide

The turbostratic nickel hydroxide [11] is prepared at room temperature by adding an ammonia solution to a nickel nitrate solution. A precipitate is obtained which is alternately washed and centrifuged several times until the pH becomes neutral; this precipitate is quickly dried at ambient temperature [12].

The green hydroxide thus obtained has a lamellar but imperfectly organized structure [12]. A detailed description of the disordered structure has been derived from X-ray diffraction studies. The X-ray diffraction pattern is shown in Fig. 1a with the diffraction pattern of crystallized β(II) $Ni(OH)_2$ given for comparison (Fig. 1b). It exhibits only two lines corresponding to 8.5 Å and 4.25 Å, respectively; there are also two dis-symetrical bands which are serrated. This type of pattern has been observed with some lamellar disordered structures such as clays [13] and carbon black [14]. The structure of the αc hydroxide can be described [12] as a stacking along the c axis of equidistant and parallel layers of nickel (II) hydroxide similar to those found in crystallized β(II) $Ni(OH)_2$ [15], but these layers are randomly oriented (Fig. 1c, d). Such a disordered structure is called a turbostratic structure [16]. According to this model, the two lines are indexed as 0 0 1 and 0 0 2 lines and are related to the regular stacking of the sheets along the c axis. The dis-symetric bands are indexed as *h k* bands and are explained by diffraction on a two-dimensional lattice.

The distance between the layers in the turbostratic hydroxide is 8.5 Å and this distance appears much larger than in the well-crystallized hydroxide structure. This is explained by the presence of a layer of intercalar water molecules linked by hydrogen bonds to the hydroxyl groups of the nickel hydroxide sheets [17, 18].

By electron microscopy [19] turbostratic nickel hydroxide appears as aggregates of thin crumpled sheets, without any definite shape (see Fig. 4a). The crystallites of the turbostratic hydroxide have a mean size of 30 Å along [0 0 1] which corresponds to a stacking of about five layers;

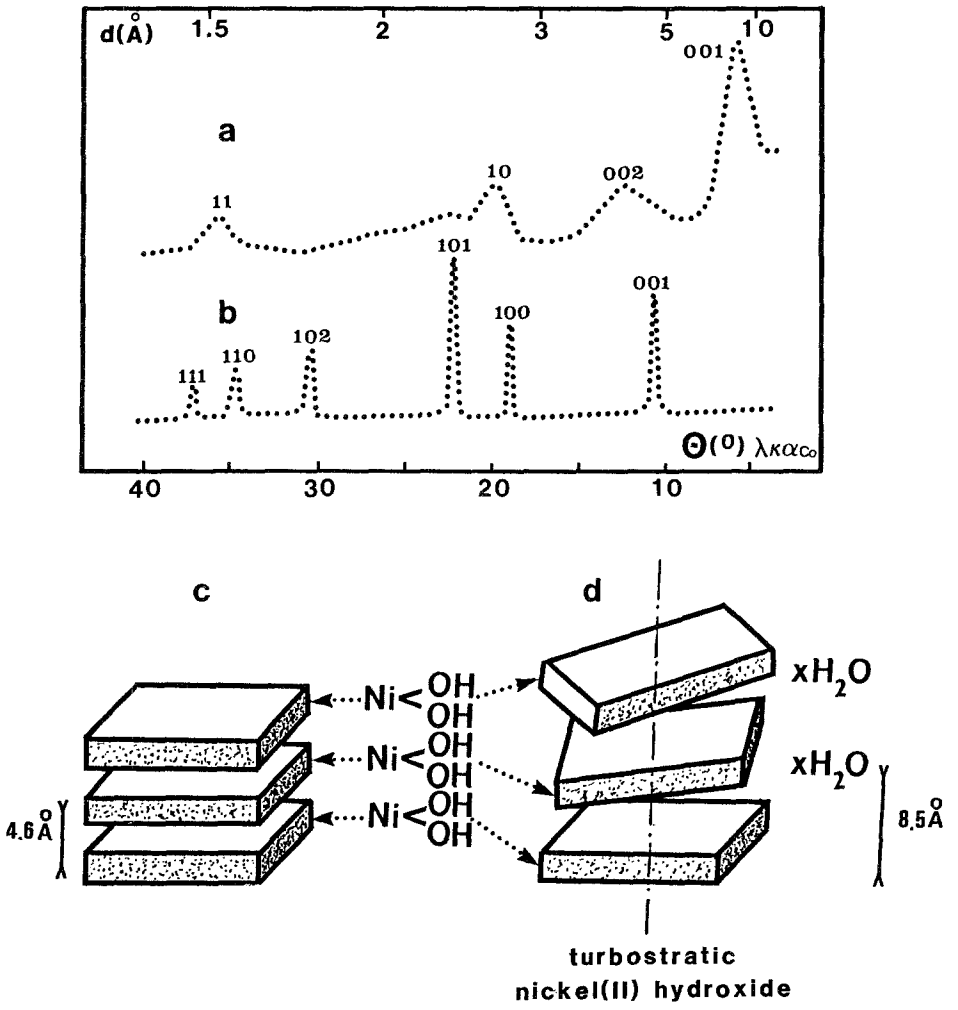

Fig. 1. X-ray diffraction patterns and structural schemes of nickel hydroxides. (a, d), Turbostratic nickel hydroxide, αc; (b, c), β(II) $Ni(OH)_2$ crystallized nickel hydroxide.

the mean size of the crystallites in the (0 0 1) plane was evaluated as 80 Å [11].

Due to the high degree of division of the turbostratic hydroxide, the presence of adsorbed species cannot be avoided and the hydroxide retains surface water and nitrate ions adsorbed during precipitation [17, 18]; the amount of nitrate ions is less than 3% [11].

Turbostratic nickel hydroxide aged completely to crystallized $Ni(OH)_2$ within a few hours in alkali solution or pure aqueous medium at room temperature. Le Bihan and Figlarz [19] have shown without any ambiguity that the mechanism of recrystallization proceeds via the solution by dissolution of the turbostratic phase and nucleation and growth of crystallized β(II) $Ni(OH)_2$ from the solution.

3. Experimental details

The turbostratic hydroxide was cycled by means of a micro-cell which simulates the working of pocket cells. After mixing the hydroxide with graphite in order to improve the conductivity inside the electrode, the powder was put between two nickel-plated steel discs, 12 mm in diameter, and compressed at $1\,t\,cm^{-2}$. The pellet thus obtained was placed into a plexiglass support with a current collector. The nickel hydroxide electrode was then plunged into a 4.5 N KOH

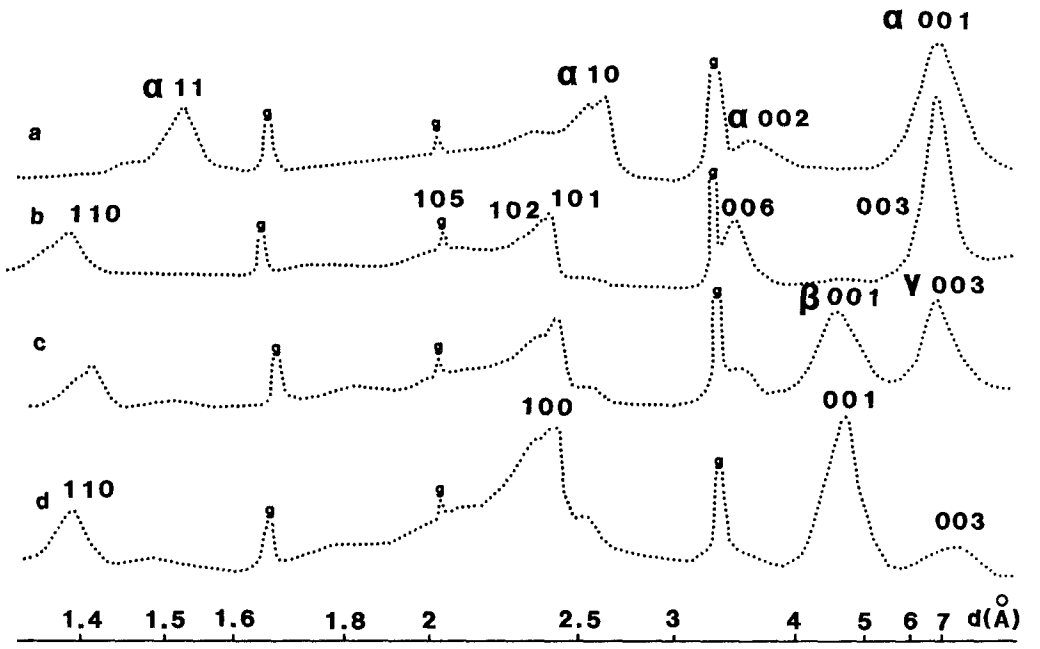

Fig. 2. X-ray diffraction patterns for the charged active materials after a variable number of cycles. (a) Uncycled turbostratic nickel hydroxide: starting material. (b) The material in the oxidized state after one or two charges: practically pure γ(III). (c) The material after three or four charges: mixture of γ(III) + β(III) (d) The material after five charges: practically pure β(III) plus very little γ(III). The graphite lines are represented by g.

solution, between two cadmium counter electrodes, and was cycled at the C/5 rate. In order to use the same conditions as for the β(II) $Ni(OH)_2$ study [1], the first two charges were performed for 20 and 15 h, respectively (compared to 7.5 h for the normal cycling conditions).

Five cycles were carried out to follow the change from the αc(II)/γ(III) to the β(II)/β(III) system. After each charge and discharge some electrodes were removed and the samples studied by X-ray diffraction and electron microscopy. Transmission electron microscopy and diffraction observations were made with a Philips EM 301 microscope and the X-ray diffraction patterns were obtained with a Philips PW 1710 diffractometer or a Guinier camera using cobalt λKα radiation.

4. Results and discussion

The discharge capacity of the active material as a function of the number of cycles is reported in Table 1. The capacity falls quickly and significantly in the initial stage of cycling. This fall in discharge acceptance of the turbostratic nickel hydroxide electrode may be related to important structural and textural modifications of the starting active material.

Figs 2 and 3 show the X-ray diffraction patterns obtained for charged and discharged samples for the first five cycles. Considering the results for charged samples, it is clear from Fig. 2 that for the first two charges the oxidized phases are γ(III), but for the following cycles the β(III) phase appears, and at the fifth cycle there is practically pure β(III) plus very little γ(III). The diffraction patterns corresponding to the discharged states (Fig. 3) indicate, rather surprisingly, that β(II) $Ni(OH)_2$ is obtained from

Table 1. Mean capacity of the turbostratic nickel hydroxide electrode for the first cycles

Number of cycles	*Mean capacity* ($mA\,h\,g^{-1}\,Ni$)
1	420
2	346
3	310
4	297

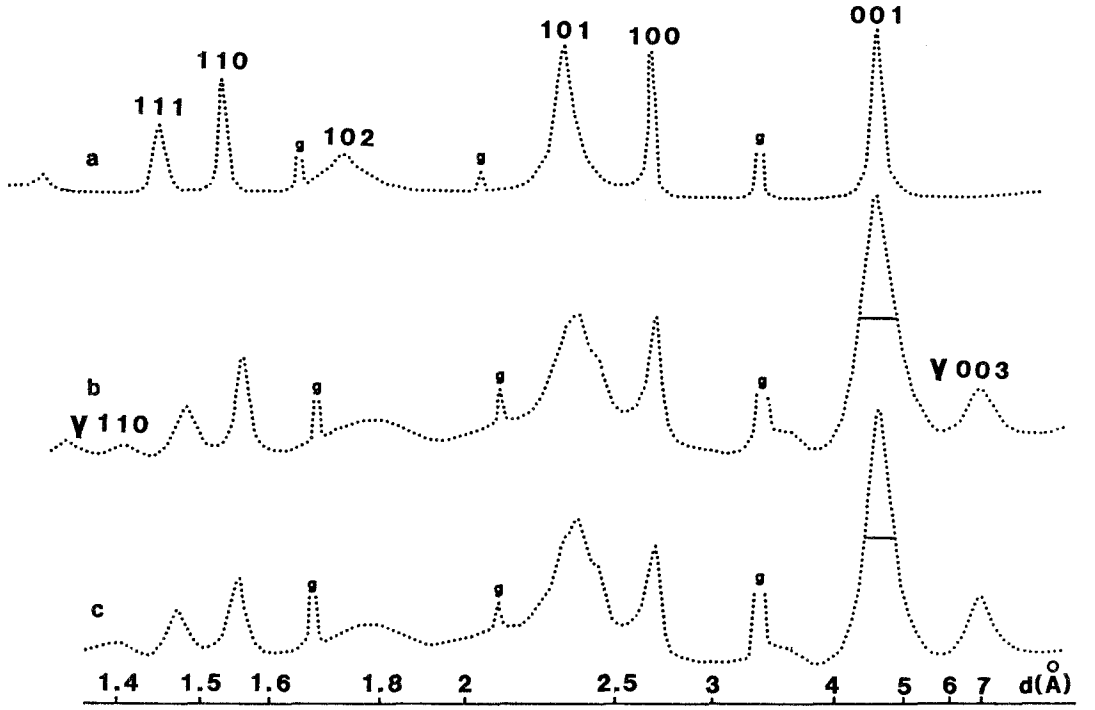

Fig. 3. X-ray diffraction patterns for the discharged material after a variable number of cycles. (a) Uncycled crystallized β(II) $Ni(OH)_2$ given for comparison (industrial sample called C2 in [1]). (b) The material at reduced state after one cycle: crystallized β(II) $Ni(OH)_2$ with broad lines and a small amount of γ(III). (c) The material at reduced state after five cycles: β(II) $Ni(OH)_2$ plus a small amount of γ(III) as in (b); note the narrowing of the 0 0 1 line compared to (b). The graphite lines are represented by g.

the first cycle with a small amount of γ(III) always present. From these results it is interesting to note that starting from turbostratic nickel hydroxide by redox cycling the αc(II)/γ(III) system is quickly converted to the β(II)/β(III) and β(II)/γ(III) phase couples, and that after five cycles only the β(II)/β(III) couple remains.

Electron microscopy completes this structural information. As indicated previously, the starting active material, i.e. the turbostratic nickel hydroxide, appears as aggregates of thin crumpled sheets (Fig. 4a). After the first charge, a mixture of thin crumpled sheets, more or less broken, and a second kind of particle which are very small and thin platelets of about 150 Å diameter and a few tens Å thick, were observed (Fig. 4b). During the first discharge of the electrode the crumpled sheets disappear, and after the complete first discharge only platelets are observed (Fig. 4c).

The behaviour of the turbostratic nickel hydroxide electrode appears rather complicated. This is due to the superposition of two kinds of phenomena: on the one hand the ageing of turbostratic nickel hydroxide and ageing of the β(II) $Ni(OH)_2$ phase formed from the turbostratic phase, on the other hand the actual oxidation and reduction reactions.

A series of questions arises which shall now be discussed: what are the transformations involved during the first charge? What is the mechanism of the first discharge reduction leading from γ(III) to β(II) and of further discharges? And finally, what is the reason for the increase of the β(III) fraction as the number of cycles increases?

4.1. *Study of the first charge*

It has been shown that during the first charge the oxidized phase obtained is γ(III) (Fig. 2b). However, turbostratic nickel hydroxide ages completely to crystallized $Ni(OH)_2$ within a few hours in alkaline solution or a pure aqueous medium at room temperature [19]. As the first

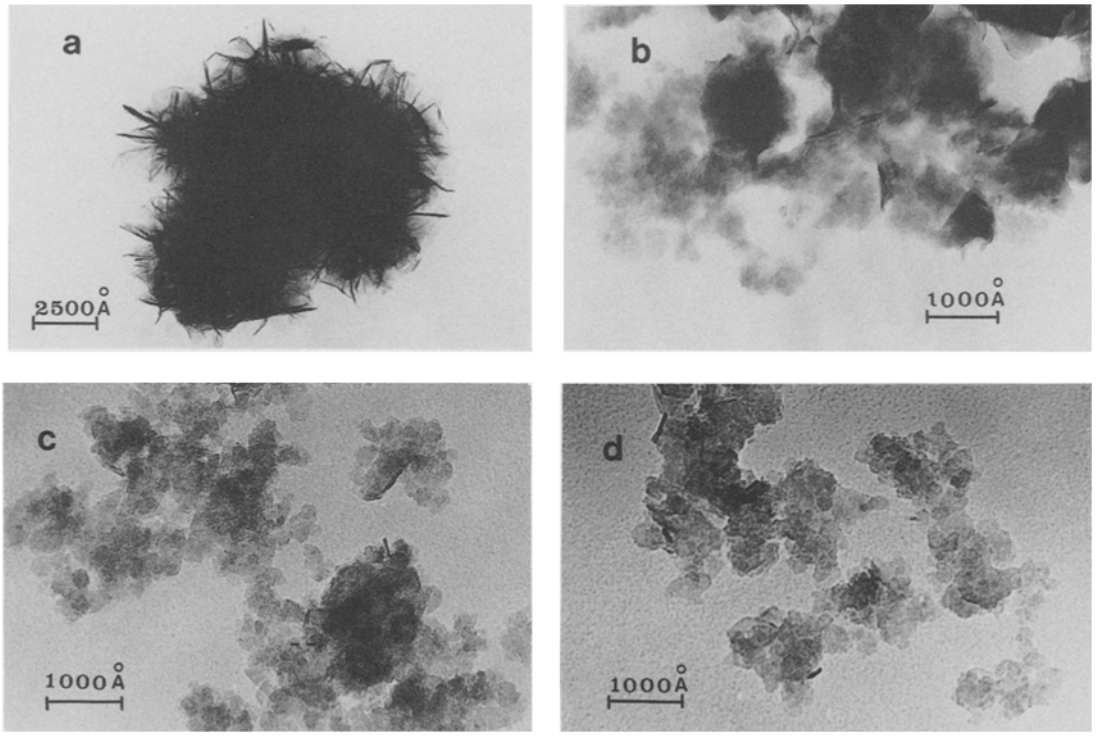

Fig. 4. Electron micrographs. (a) Uncycled turbostratic nickel (II) hydroxide: the starting material appears as aggregates of thin crumpled sheets. (b) The material in the oxidized state after one charge: a mixture of crumpled sheets more or less broken (alpha-generated γ(III)) and small and thin hexagonal platelets (beta-generated γ(III)). (c) The material in the reduced state after one cycle: small platelets of β(II) $Ni(OH)_2$. (d) Alpha-generated β(II) $Ni(OH)_2$ prepared by ageing turbostratic nickel (II) hydroxide in 4.5 N KOH at 20° C: small platelets with a mean diameter of 200 Å and a thickness of 40 Å.

charge is performed in 20 h it is therefore justified to make the assumption that two reactions can compete: the ageing of the turbostratic hydroxide

$$\alpha c(II) \longrightarrow \beta(II)$$

and the direct oxidation

$$\alpha c(II) \longrightarrow \gamma(III)$$

In order to verify this hypothesis, samples were taken during the course of galvanostatic charge and examined by X-ray diffraction and electron microscopy. As an example, a sample submitted to 2 h oxidation was characterized by X-ray diffraction as a mixture of αc(II), γ(III) and β(II); the largest part of the mixture is β(II) (Fig. 5a). Electron microscopy shows the presence of crumpled sheets of the turbostratic nickel (II) hydroxide with broken crumpled sheets of the γ(III) phase and small platelets of β(II) hydroxide.

Another confirmation of the occurrence of the $\alpha c(II) \rightarrow \beta(II) \rightarrow \gamma(III)$ path is given by the reproduction of the $\beta(II) \rightarrow \gamma(III)$ step. With this objective, a sample of β(II) ex αc (alpha-generated β(II)) was prepared by ageing turbostratic nickel hydroxide in 4.5 N KOH at 20° C for 20 h. The X-ray diffraction pattern is reported in Fig. 5b; electron microscopy shows that this hydroxide consists of small platelets 150–250 Å in diameter and 30–50 Å thick (Fig. 4d). This alphagenerated β(II) hydroxide was submitted to electrochemical oxidation under exactly the same conditions as the turbostratic nickel hydroxide; the resulting product is pure γ(III) (Fig. 5c). This study confirms the fact that the first charge proceeds via two paths as shown schematically in Fig. 6.

The $\alpha c(II) \rightarrow \gamma(III)$ reaction is the direct oxidation of the turbostratic nickel hydroxide. Electron microscopy shows that the oxidation is related to the breaking up of the turbostratic

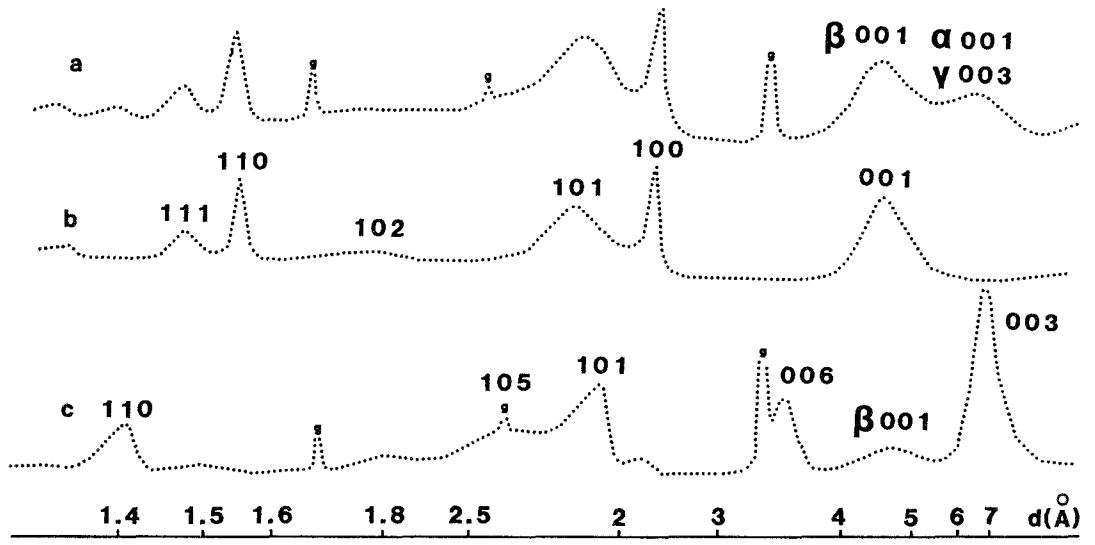

Fig. 5. X-ray diffraction patterns. (a) Turbostratic nickel (II) hydroxide submitted to 2 h oxidation at the C/5 rate: mixture of α(II)/γ(III) + β(II) in majority proportion. (b) Alpha-generated β(II) $Ni(OH)_2$ prepared by ageing turbostratic nickel (II) hydroxide in 4.5 N KOH at 20° C. (c) γ(III) obtained by oxidation of the previous alpha-generated β(II) at the C/5 rate for 20 h. The graphite lines are represented by g.

hydroxide sheets. This result can be interpreted by assuming that oxidation induces some strains in relation to the large difference of the nickel–nickel distance in the (0 0 1) planes in the oxidized NiOOH γ-phase and in the turbostratic hydroxide; these strains are relieved by sheet fragmentation [20].

The second path of the oxidation reaction consists of two steps. The first one is the ageing of turbostratic nickel hydroxide which proceeds by dissolution of the turbostratic phase and nucleation-growth of crystallized β(II) $Ni(OH)_2$ from solution [11]. This step plays a major role in the first charge. The β(II) hydroxide thus produced is itself oxidized to γ(III). This last reaction is pseudomorphous and, as will be

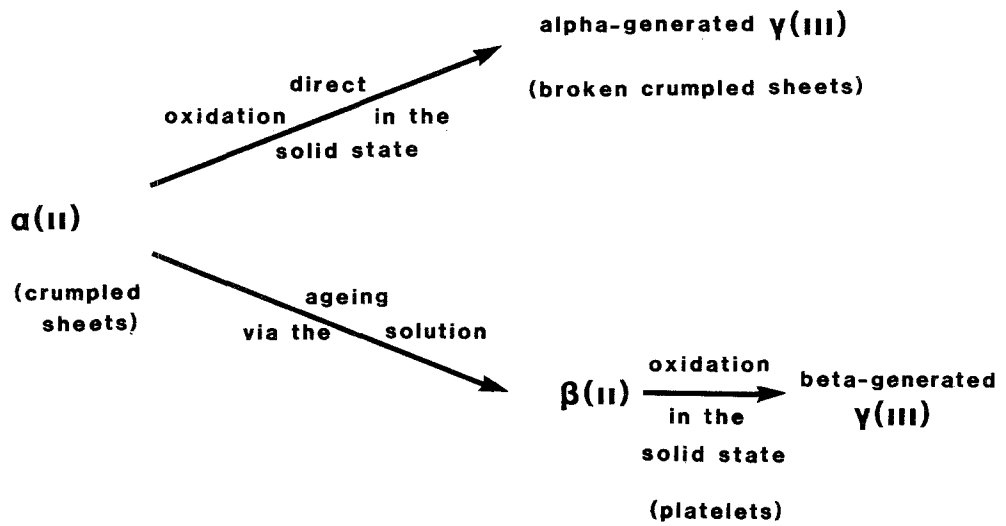

Fig. 6. Scheme illustrating the reactions which compete during the first charge of turbostratic nickel (II) hydroxide.

discussed later, this direct oxidation of β(II) to γ(III) implies that certain conditions are fulfilled (cf. section 4.3). It should be stressed that the direct oxidation β(II) $\rightarrow$ γ(III) has never before been established and constitutes a new route in the study of the electrochemical cycling of nickel hydroxide electrodes.

4.2. *Study of the discharge mechansm*

The discharge mechanism of the γ(III) phase can be explained largely on the basis of structural and textural filiations in the course of the reaction.

The resulting product of the first charge is γ(III) (Fig. 2b), and by electrochemical reduction one obtains the β(II) phase at the end of first discharge (Fig. 3b). Nevertheless, it must not be concluded that the discharge proceeds simply by the reaction γ(III) $\rightarrow$ β(II). Indeed, it has been shown previously that γ(III) genesis has two origins, the α(II) and β(II) phases, and that γ(III) has two different morphological characteristics, alpha-generated γ(III) in the form of broken crumpled sheets and beta-generated γ(III) in the form of small platelets. In other respects the β(II) phase obtained at the end of the first discharge consists only of one kind of particle, i.e. small platelets. This means that the crumpled sheets of the alpha-generated γ(III) have been completely converted into platelets. Such a textural change is experimental evidence for a reaction mechanism via the solution rather than a solid–solid reaction. Such a mechanism supposes the occurrence of a soluble species which cannot be the γ(III) phase; in fact γ(III) is very stable in KOH medium and remains stable when submitted to prolonged overcharging at the C/100 rate for 24 h. This suggests that the discharge mechanism might be

$$\gamma(\mathrm{III}) \longrightarrow \alpha\mathrm{c(II)} \longrightarrow \beta(\mathrm{II}).$$

The results obtained for the discharge mechanism can be represented schematically as shown in Fig. 7.

The reduction of beta-generated γ(III) is the direct reduction of γ(III) to β(II) and presents the same characteristics as the direct oxidation β(II) $\rightarrow$ γ(III) (cf. Sections 4.1 and 4.3).

The reduction of alpha-generated γ(III) is a two-step reaction, the first step being the reduction γ(III) $\rightarrow$ α(II) which is a solid-state pseudomorphous reaction, and the second being the ageing of the turbostratic nickel (II) hydroxide, obtained by reduction, via the solution to β(II) $Ni(OH)_2$.

During further discharge the alpha-generated γ(III) has disappeared and the discharge mechanism is limited to the reduction of beta-generated γ(III) as far as this phase still exists.

4.3. *Oxidation mechanism of alpha-generated β(II) nickel hydroxide*

From the second cycle the oxidized phase is beta-generated γ(III), but as the number of cycles

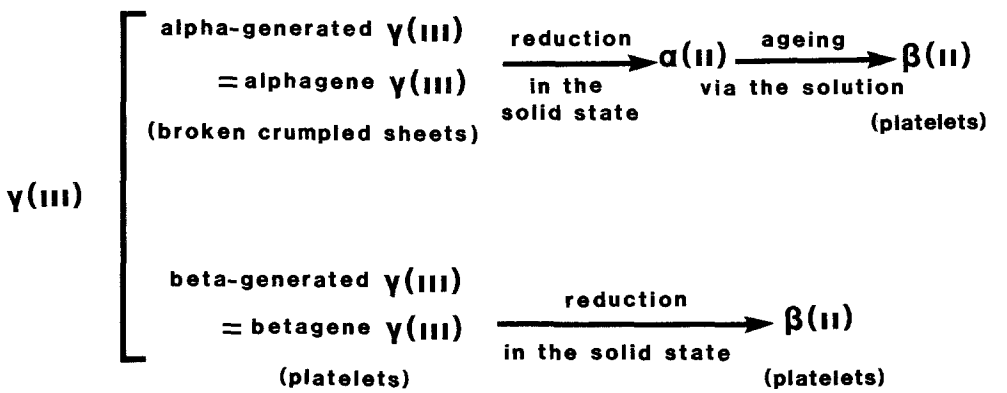

Fig. 7. Diagrammatic representation of the discharging process ('alphagene' or 'betagene' denotes phases that produce alpha or beta phases).

increases the oxidized state becomes a mixture of γ(III) and β(III) with a proportion of γ(III) which decreases (Fig. 2). As the reduced state is β(II), this implies two oxidation reactions:

$$\beta(II) \xrightarrow{(1)} \gamma(III)$$

and

$$\beta(II) \xrightarrow{(2)} \beta(III)$$

In other respects the β(II) discharged state consists of only one kind of particle: small hexagonal platelets with a diameter of about 100–200 Å and a thickness of 30–50 Å.

Two questions arise. What is the driving force which makes the system swing from reaction 1 to reaction 2? What is the difference between the betagene β(II) and gammagene β(II) particles? It is not possible to answer the last question by an electron microscopy study of β(II) because it is very difficult to disperse the small and thin β(II) platelets. Fortunately, it is possible to find an answer to the question from the X-ray diffraction patterns of β(II) phases. Indeed, as the number of cycles increases, a decrease of the width at half maximum intensity of the 0 0 1 line of β(II) is observed (Table 2). This means that the crystallite size of the particles increases in the [0 0 1] direction, i.e. the thickness of the platelets which are lying on the (0 0 1) plane increases.

There is therefore a clear correlation between the thickness of the particles and their ability to oxidize into the γ(III) or β(III) phases. When the thickness is below a critical value the β(II) particles are gammagene towards oxidation; when the particles are thicker they are betagene. This can be explained from structural considerations on the β(II), β(III) and γ(III) phases. The oxidized nickel hydroxides present two types of phase, both with a lamellar structure which differ in interlayer spacing and composition [9, 10, 21]. The structure of the β(III) NiOOH phase is closely related to β(II) $Ni(OH)_2$ from which it derives owing to disintercalation of one proton and one electron. It crystallizes in the hexagonal system with $a = 2.82$ Å and $c = 4.85$ Å compared to $a = 3.13$ Å and $c = 4.60$ Å for β(II) $Ni(OH)_2$. The γ(III) phases are lamellar with layers of the same composition as β(III) NiOOH, but water and alkaline ions in variable amount are intercalated between the layers. The interlamellar spacing is about 7 Å and the unit cell is triple with $a = 2.82$ Å and $c \sim 21$ Å.

Starting from β(II) $Ni(OH)_2$, the transformation to γ(III) induces strains within the particles [1, 20]. Those due to the difference in the nickel–nickel distances in the oxidized and reduced phases are easily accommodated because of the very small size of the particles. The strains induced by the very large difference in interlamellar spacing along the c axis between γ(III) and β(II) are more readily relaxed as the number of planes in the [0 0 1] direction is small, i.e. the platelet particles are thinner. For thicker particles, the β(II) $\rightarrow$ β(III) transformation is promoted in order to minimize the induced strains along [0 0 1].

The swing from reaction 1 to reaction 2 is due to the ageing of β(II) particles which increase in thickness as indicated by the narrowing of the 0 0 1 X-ray diffraction line (Table 2). This ageing process can be related to the well-known Oswald ripening phenomenon [22, 23]. Once again this ageing effect occurs via the solution: the thinner particles dissolve and a growth of the other particles is observed, growth which is fed from the solution. The different phenomena which occur in the oxidation process of alpha-generated β(II) are shown schematically in Fig. 8.

It must be emphasized that the mechanism which has been established for the chemical and electrochemical redox of 'common' β(II) $Ni(OH)_2$ (cf. Introduction) does not seem to work here in the case of alphagenerated β(II). For 'common' β(II) hydroxide it has been shown that starting from an hydroxide with a monolithic texture, the redox cycling produces a mosaic texture [1]. In the case of alpha-generated

Table 2. Width at half maximum intensity for the 0 0 1 line of β(II) $Ni(OH)_2$ obtained after a variable number of cycles

Number of cycles	*0 0 1 width at half maximum intensity* $^\circ 2\theta \times 10^3$ *(radians)*
1	52
2	52
3	44
4	44
5	42

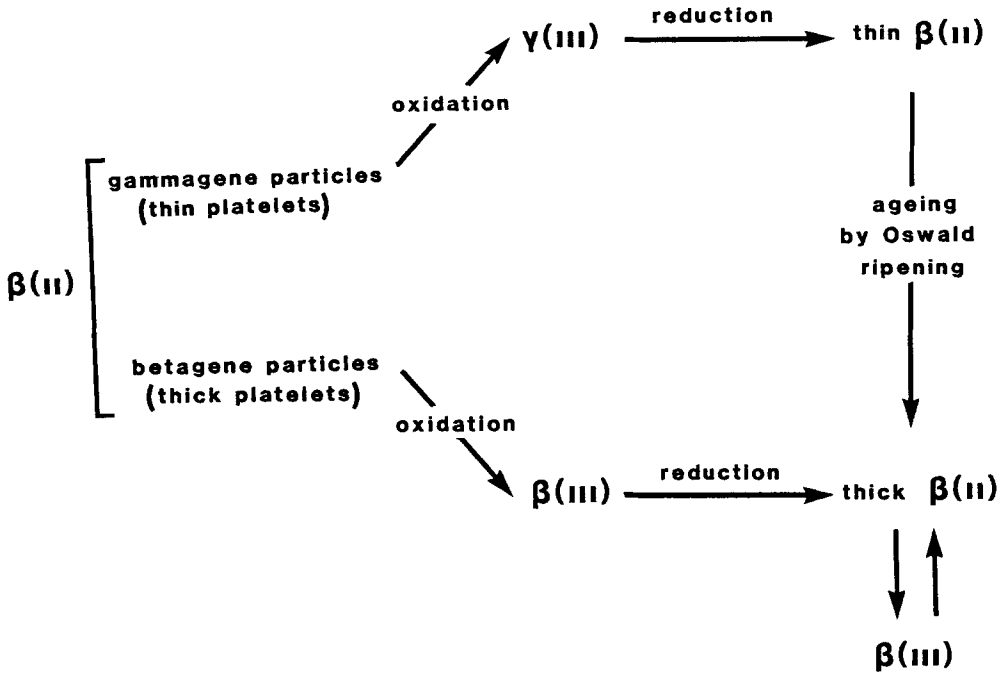

Fig. 8. Schematic representation of the oxidation mechanism of alpha-generated β(II) $Ni(OH)_2$.

hydroxide the particles are monolithic too, but broadening of the X-ray diffraction lines indicating the formation of a mosaic texture is not observed. This can be related to the fact that the particles of alpha-generated β(II) are much smaller than those of 'common' β(II). Due to the large surface to volume ratio, the strains produced by the reaction can be accommodated by the particles without any textural modification. There probably exists a critical value for the crystallite size under which the monolithic to mosaic texture transformation does not occur.

Acknowledgements

The authors wish to thank the 'Ministère de la Recherche et de la Technologie' who sponsored this study and 'SAFT' for permission to publish this work.

References

[1] A. Delahaye-Vidal, B. Beaudoin and M. Figlarz, *Reactivity of Solids* **2** (1986) 223.
[2] P. Oliva, J. Leonardi, J. F. Laurent, C. Delmas, J. J. Braconnier, M. Figlarz, F. Fievet and A. de Guibert, *J. Power Sources* **8** (1982) 229.
[3] N. Yu Uflyand, A. M. Novakovski, Yu. M. Pozin and S. A. Rozentsveig, *Elektrokhimiya* **2** (1966) 234.
[4] *Idem, ibid.* **3** (1967) 537.
[5] R. Barnard, G. T. Crickmore, J. A. Lee and F. L. Tye, *J. Appl. Electrochem.* **10** (1980) 61.
[6] R. Barnard, C. F. Randell and F. L. Tye, *J. Electroanal. Chem.* **119** (1981) 17.
[7] *Idem, Power Sources*, Vol. 8, Academic Press, London (1981) p. 401.
[8] G. W. D. Briggs and W. F. K. Wynne-Jones, *Electrochim. Acta* **7** (1962) 241.
[9] H. Bode, K. Dehmelt and J. Witte, *ibid.* **11** (1966) 1079.
[10] *Idem, Z. Anorg. Allg. Chem.* **366** (1969) 1.
[11] S. Le Bihan, Thèse, Paris, 1974, N° CNRS AO 9424.
[12] S. Le Bihan, J. Guenot and M. Figlarz, *C.R. Acad. Sci. C* **270** (1970) 2131.
[13] J. Mering and J. Maire, 'Les Carbones', Masson, Paris (1965) p. 129.
[14] D. MacEwan, in 'The X-ray identification and Crystal Structure of Clay Minerals' (edited by G. Brown), Mineralogical Society, London (1961) p. 143.
[15] J. Deportes, P. Mollard, J. Penelon, S. Le Bihan and M. Figlarz, *C.R. Acad. Sci. B* **272** (1971) 449.
[16] J. Biscoe and B. E. Warren, *J. Appl. Phys.* **13** (1942) 364.
[17] M. Figlarz and S. Le Bihan, *C.R. Acad. Sci. C* **272** (1971) 580.

[18] *Idem, Thermochim. Acta* **6** (1973) 319.
[19] S. Le Bihan and M. Figlarz, *J. Cryst. Growth* **13/14** (1972) 458.
[20] B. Beaudoin, E. Khiar, A. Vidal and M. Figlarz, in 'Reactivity of Solids', Materials Science Monographs 28B (edited by P. Barret and L. C. Dufour), Elsevier, Amsterdam (1985) p. 503.
[21] O. Glemser and J. Einerhand, *Z. Anorg. Allg. Chem.* **261** (1950) 26.
[22] W. Oswald, *Z. Phys. Chem.* **34** (1900) 495.
[23] R. Liesegang, *ibid.* **70** (1910) 374.